

Communication

# ZnCl<sub>2</sub>-Enhanced Intrinsic Luminescence of Tin Chlorophosphate Glasses

Ting Wu <sup>1,2</sup>, Yiting Tao <sup>1,2</sup>, Panting Wang <sup>1,2</sup>, Mingjun Zhao <sup>1,2</sup> and Danping Chen <sup>1,\*</sup> 

<sup>1</sup> Key Laboratory of Materials for High Power Laser, Shanghai Institute of Optics and Fine Mechanics, Chinese Academy of Sciences, Shanghai 201800, China

<sup>2</sup> Center of Materials Science and Optoelectronics Engineering, University of Chinese Academy of Sciences, Beijing 100049, China

\* Correspondence: d-chen@mail.siom.ac.cn

**Abstract:** This communication reports the intrinsic luminescence of tin chlorophosphate glasses. The glass maintains the low melting point characteristics of tin fluorophosphate glasses, and exhibits a red-shifted and broadened excitation wavelength peak. Tin chlorophosphate glasses can exhibit a broadband luminescence of 400–700 nm under an excitation of 380–430 nm. Furthermore, the introduction of ZnCl<sub>2</sub> into tin chlorophosphate glasses can considerably enhance the luminescence without affecting their low-melting characteristics. The luminescence intensity can be increased fourfold, with the enhancement attributed to the reduced visible absorption, improved dispersion of Sn<sup>2+</sup> ions, and the energy exchange between Sn<sup>2+</sup> and Zn<sup>2+</sup> in the glasses owing to the addition of ZnCl<sub>2</sub>.

**Keywords:** low-melting point; tin-chlorophosphate glasses; luminescence; ZnCl<sub>2</sub>



**Citation:** Wu, T.; Tao, Y.; Wang, P.; Zhao, M.; Chen, D. ZnCl<sub>2</sub>-Enhanced Intrinsic Luminescence of Tin Chlorophosphate Glasses. *Photonics* **2022**, *9*, 973. <https://doi.org/10.3390/photonics9120973>

Received: 15 November 2022

Accepted: 9 December 2022

Published: 12 December 2022

**Publisher's Note:** MDPI stays neutral with regard to jurisdictional claims in published maps and institutional affiliations.



**Copyright:** © 2022 by the authors. Licensee MDPI, Basel, Switzerland. This article is an open access article distributed under the terms and conditions of the Creative Commons Attribution (CC BY) license (<https://creativecommons.org/licenses/by/4.0/>).

## 1. Introduction

The tin fluorophosphate system is a well-known glass system with a low glass transition temperature ( $T_g$ ); it also prevents the degradation in the luminous efficacy of white light-emitting diodes (WLEDs) and color shift due to aging and yellowing, compared with traditional encapsulation materials such as organic silicone or resin [1–3]. Moreover, tin-containing glasses are considered to be excellent substrates for the preparation of white fluorescent glasses, and the Sn<sup>2+</sup> activation center can exhibit broadband blue-green emissions with a short lifetime and high quantum efficiency [4]. Sn<sup>2+</sup> acts as a ns<sup>2</sup>-type ( $n \geq 4$ ) emission center and exhibits an s-p parity-permissive transition, the emission properties of which strongly depend on the local coordination states of Sn, because the s and p electrons are in the outermost layers in the ground state (ns<sup>2</sup>) and the excited state (ns<sup>1</sup> np<sup>1</sup>) [5–7].

Wang et al. [8] reported that Sn-P-O-F (TFP) glasses without rare-earth elements can exhibit an intrinsic broadband visible emission under excitation of a 325 nm wavelength, but these glasses could not be used as the light source for LED excitation because the wavelength was too short. Subsequently, active ions such as Mn<sup>2+</sup> or Eu<sup>3+</sup> were doped into TFP host glasses to achieve a tunable white-light emission [9,10]. Because of the low-melting point of TFP glasses, SrSi<sub>2</sub>O<sub>2</sub>N<sub>2</sub>: Eu<sup>2+</sup> and CaAlSiN<sub>3</sub>: Eu<sup>2+</sup> phosphors were added to achieve the full-spectrum emission of visible light under 370 nm excitation [11]. Low-melting glass is also considered an ideal solid host for organic chromophores, which includes the incorporation of Rhodamine 6G to prepare glass-organic luminophore composites [12]. Recently, Sn-P-O-Cl (TCP) glasses with a  $T_g$  lower than 200 °C, which replaced F with Cl and melted below 400 °C, were reported [13]. Because of the different electronegativities of F and Cl, it can be expected that Cl will change the nearby environment of Sn<sup>2+</sup>. On the other hand, ZnCl<sub>2</sub> is a luminescent material with a low melting point; its introduction may lead to some changes in the luminescence properties and improve the

luminescence intensity. Therefore, this paper will report the spectral properties of TCP glasses and the effect of  $\text{ZnCl}_2$  concentration on the fluorescence of TCP glasses.

## 2. Materials and Methods

### 2.1. Sample Preparation

A series of  $x \text{P}_2\text{O}_5 - (100-x) \text{SnCl}_2$  ( $x = 30, 35, 40,$  and  $50$  mol%) and  $35\text{P}_2\text{O}_5 - (65-y) \text{SnCl}_2 - y \text{ZnCl}_2$  glasses ( $y = 10, 20, 30,$  and  $40$  mol%) were melted at  $350$  °C, then quickly cooled to glass and labeled as TCP30, TCP35, TCP40, and TCP50, as well as TCPZ1, TCPZ2, TCPZ3, and TCPZ4, respectively. The raw materials were  $\text{NH}_4\text{H}_2\text{PO}_4$  (>99%, Sinopharm Chemical Reagent Co., Ltd., Shanghai, China),  $\text{SnCl}_2$  (99.95%, Shanghai Macklin Biochemical Co., Ltd., Shanghai, China), and  $\text{ZnCl}_2$  (99.9%, Shanghai Macklin Biochemical Co., Ltd.). Well-mixed 25 g batches of the raw materials were placed in a covered alumina crucible and melted at  $350$  °C for 10 min. The melts were then quickly poured onto preheated graphite molds and annealed in a muffle furnace at temperatures approximately equal to their glass transition temperatures. All samples were cooled to room temperature, cut, and optically polished for the subsequent tests. Since the alumina crucible may introduce  $\text{Al}^{3+}$  into the glass liquid during the melting process, the composition of P, Sn, and Al elements in the glass was quantitatively measured by ICP-MS. At the melting temperature of  $350$  °C, the content of Al introduced by the alumina crucible in the sample does not exceed 0.1 wt %. Therefore, the influence of  $\text{Al}^{3+}$  ions in the glass is negligible.

### 2.2. Characterization

Absorption spectra were obtained using a PerkinElmer Lambda 950 UV/VIS/NIR spectrophotometer in the range of 300–800 nm. PL and PLE spectra and the emission decay were measured using a high-resolution spectrofluorometer (Edinburgh Instruments FLS 920, UK). The glass transition temperature ( $T_g$ ) was determined by a Netzsch STA449/C differential scanning calorimeter (DSC) at a heating rate of 5 K/min. Raman spectra were measured using a Renishaw In Via Raman microscope in the range of 100–1400  $\text{cm}^{-1}$  using a 785 nm excitation line. All measurements were performed at room temperature.

## 3. Results and Discussion

### 3.1. Spectral Properties of Binary TCP Glasses

Figure 1a shows the absorption spectra of the TCP glasses. Compared to traditional phosphate glasses, the absorption edge of TCP glasses red-shifts with increasing  $\text{SnCl}_2$  content, which is due to the strong absorption band of Sn in the band gap of the host tin chlorophosphate glasses [8]. The illustration shows the energy transfer process from the excitation to the emission of  $\text{Sn}^{2+}$ , and reveals the energy transfer of the triplet (T1)-singlet (S1) relaxation band model of the  $\text{Sn}^{2+}$  activator [14]. The excited states include two energy bands: the high-energy state S1 and the low-energy state S1'. Between the excited states of S1/S1' and ground state S0, there is a triple-merged emission band T1. The  $\text{Sn}^{2+}$  ions in S0 are transferred to the excited state by absorbing photons through the following process:  $\text{S0} + h\nu \rightarrow \text{S1/S1}'$ . The  $\text{Sn}^{2+}$  ions in the excited states are transferred to T1 by nonradiative transitions, and the transition probability is dependent on the Sn concentration and the glass structure [15]. Therefore, there are two emission methods in TCP glasses:  $\text{S1/S1}' \rightarrow \text{S0}$  ( $\alpha$ -band, ~450 nm) and  $\text{T1} \rightarrow \text{S0}$  ( $\beta$ -band, ~530 nm). Figure 1b shows the PLE spectra of the TCP glasses under 530 nm excitation, which consist of short and long absorption bands. The short band remains almost unchanged around 275 nm, which may be the luminescence of  $\text{Sn}^{2+}$  in the pure oxidation environment of the phosphate network; its intensity decreases with increasing  $\text{SnCl}_2$  content [4,16]. The long band is due to the  $\text{S0} \rightarrow \text{S1}'$  absorption transition of  $\text{Sn}^{2+}$ , and presents a red shift with increasing  $\text{SnCl}_2$  content. The excited-state S1' with lower energy is not only strongly dependent on the  $\text{Sn}^{2+}$  concentration but is also affected by the local structure of  $\text{Sn}^{2+}$  [8]. Because some Sn-O and P-O bonds are replaced by Sn-Cl and P-Cl bonds with increasing  $\text{SnCl}_2$  concentration and the electronegativity of Cl is lower than that of O, the covalency of Sn-Cl bonds is higher,

which narrows the optical energy bandgap, resulting in a red shift in the absorption and excitation spectra. On the other hand, the covalency of Sn-Cl is also higher than that of Sn-F; therefore, compared with Sn-P-O-F glasses, the absorption and excitation wavelengths of the TCP glasses are red-shifted, and the excitation bands render the glasses suitable for application as ultraviolet/visible LED light sources.

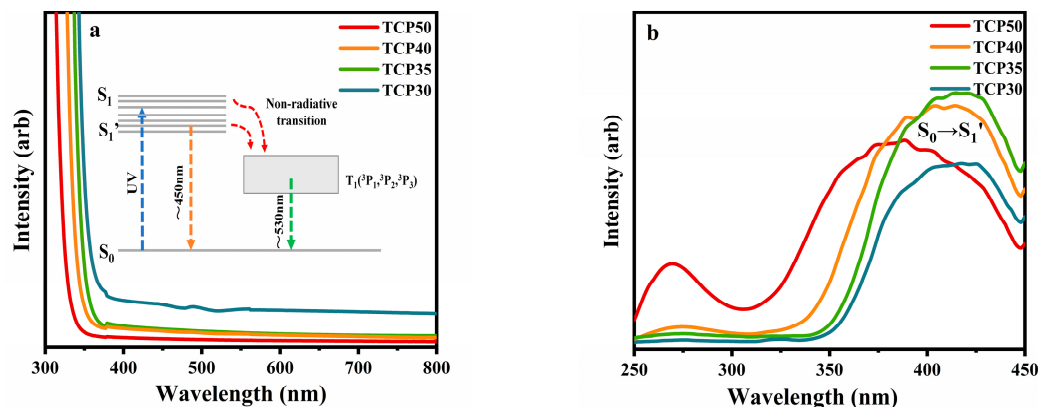


Figure 1. (a) Absorption spectra of TCP glasses, inset: Sn<sup>2+</sup> energy transfer model; (b) PLE spectra of TCP glasses under 530 nm excitation.

Figure 2a shows the PL spectra of the TCP glasses when the excitation wavelength is 390 nm; an ultralong broadband emission of 400–700 nm is observed, which is characteristic of s-p parity-allowed ns<sup>2</sup>-type emission centers. It consists of α- and β-bands and is strongly influenced by the surrounding coordination field. The PL spectra were deconvoluted into two bands using a Gaussian function (Table 1). The α- and β-bands are located at ~450 and ~530 nm. Figure 2b shows the β-peak area ratio β / (α + β) and the position of the β-peak as a function of the Sn/P molar ratio. The red shifts of the two peaks are different with the increasing Sn/P ratio; the β-peak shifts from 504 to 540 nm, and the peak area ratio shows an increasing trend. When Sn/P < 1, the fluorescence intensity of the TCP glass increases gradually with the increasing Sn/P ratio, and that for Sn/P ≈ 1 (TCP 35) is the highest. A previous study [17] indicated that Sn<sup>2+</sup> ions act as activators and participate in the formation of glass networks. From the composition and structural analysis of TCP glasses [13], when Sn/P < 1, some Sn atoms form P-O-Sn bonds in the glass network, and some Sn<sup>2+</sup> is activated to promote the luminescence of TCP glasses. When Sn/P > 1 (TCP 30), numerous Cl-Sn-Cl bonds form clusters of SnCl<sub>2</sub> in the glass, and the cross-relaxation of α-bands in the glass is increased, resulting in concentration quenching effects that reduce the luminescence intensity. From the perspective of ion spacing, at lower Sn<sup>2+</sup> concentrations, the probability of energy cross-relaxation is lower; hence, the electrons in the excited states of S<sub>1</sub> and S<sub>1</sub>' rarely transition to the T energy level, and the luminescence of the β-bands is weak. At higher Sn<sup>2+</sup> concentrations, the energy cross-relaxation increases, thereby enhancing the luminescence of the β-bands.

Table 1. Emission peak performance parameters of TCP glasses with different Sn/P ratios.

Sample	Emission Peak Position (nm)		Fluorescence Decay (ns)	β / (α + β) (%)
	α-Band	β-Band		
TCP50	435	504	2.61/20.03	56.4%
TCP40	444	518	2.39	57%
TCP35	452	520	2.30	61%
TCP30	463	540	2.37	78%

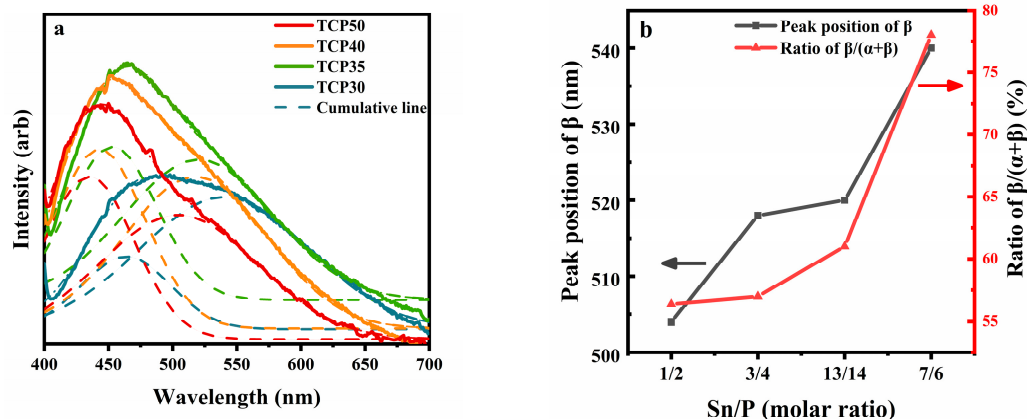


Figure 2. (a) PL spectra of TCP glasses. Two emission peaks obtained by Gaussian fitting are marked: (b) Peak area ratio  $\beta/(\alpha + \beta)$  and peak position in the  $\beta$ -band as a function of the P/Sn ratio.

The fluorescence decay curves of TCP glasses under 390 nm excitation are shown in Figure 3, and the measured fluorescence decays of the glasses are listed in Table 1. The fluorescence decays decrease slightly with increasing SnCl<sub>2</sub> content. The fast decay coefficients of the TCP samples are ~2.5 ns. However, the samples of TCP50 have two decay coefficients of 2.5 ns and 20 ns, which may be due to the influence of oxygen vacancy defects in the glasses [17].

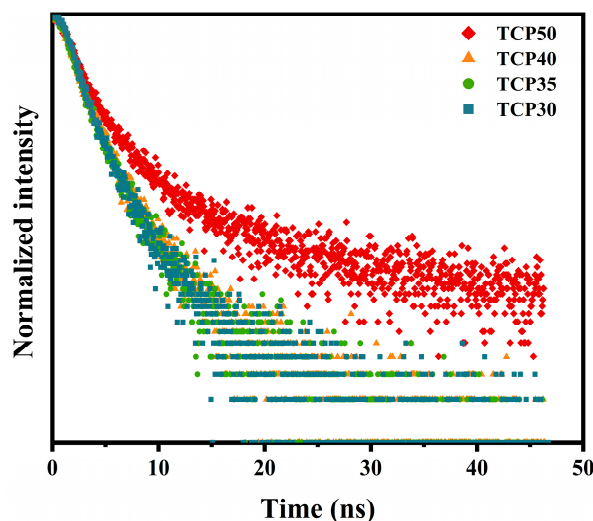


Figure 3. Fluorescence decay curve of TCPZ glasses at 530 nm.

### 3.2. Spectral Properties of Ternary P<sub>2</sub>O<sub>5</sub>-SnCl<sub>2</sub>-ZnCl<sub>2</sub> Glasses

Compounds of Zn<sup>2+</sup> are often used as low-melting-point luminescent materials. To maintain a low melting point and improve the luminescence of the glass, ZnCl<sub>2</sub> was added to the TCP glass. The luminescence of Sn-Zn co-doped glasses has been extensively studied in oxide glasses [4,6,18,19]; however, the content of SnO is often low because of the concentration quenching effect. Herein, the tin-zinc chlorophosphate (TCPZ) glasses exhibited different luminescent properties.

A stable ternary TCPZ glass was obtained at the same melting temperature of 350 °C. Figure 4a shows DSC curves of all the TCPZ glasses, their  $T_g$  increased with an increase in the ZnCl<sub>2</sub> content. Compared with TCP glasses, the  $T_g$  of TCPZ glasses did not change significantly [13]. The  $T_g$  of TCPZ glasses is less than 200 °C and still maintains the characteristics of low melting point glass. Figure 4b shows the Raman spectrum of TCPZ glasses and TCP35 glasses. In the high-frequency region of the Raman spectra, the peak at

approximately  $1103\text{ cm}^{-1}$  corresponds to the P-O symmetric stretching of the metaphosphate  $Q_2$  unit [20], and the peak at approximately  $1051\text{ cm}^{-1}$  was attributed to the P-O symmetric stretching vibration of the pyrophosphate  $Q_1$  unit [8]. The weak vibrational peak near  $978\text{ cm}^{-1}$  was assigned to the P-O vibration of  $Q_0$  [21]. The vibrational peak located near  $736\text{ cm}^{-1}$  is associated with the symmetric stretching mode of P-O-P [8]. The peak at approximately  $240\text{ cm}^{-1}$  corresponds to the Sn-O-Sn bond and asymmetric stretching vibration of the Sn-Cl-Sn bond [22,23]. There is no significant change in the vibration of the phosphorus-oxygen unit with the incorporation of Zn. The vibration peak of Sn-O/Sn-Cl bonds moves slightly to the high frequency and the vibration intensity weakens with increasing  $\text{Zn}^{2+}$  content, which is due to the gradual appearance of Zn-Cl bonds in the TCPZ glasses with the incorporation of Zn.

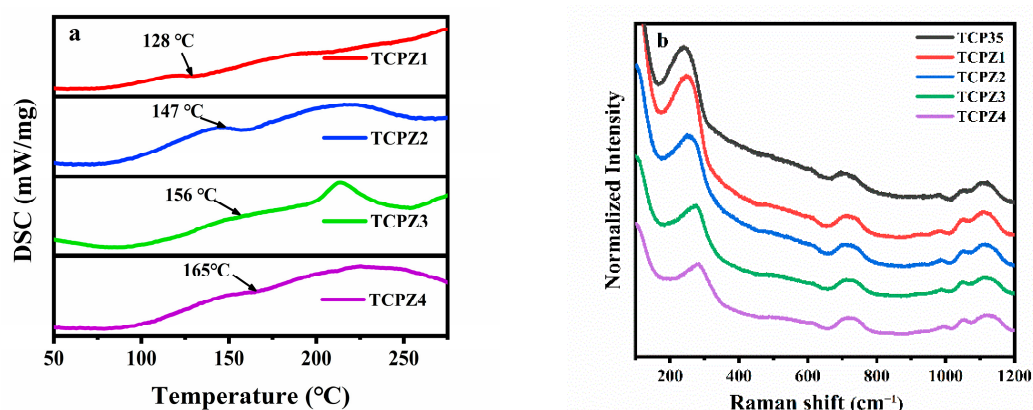
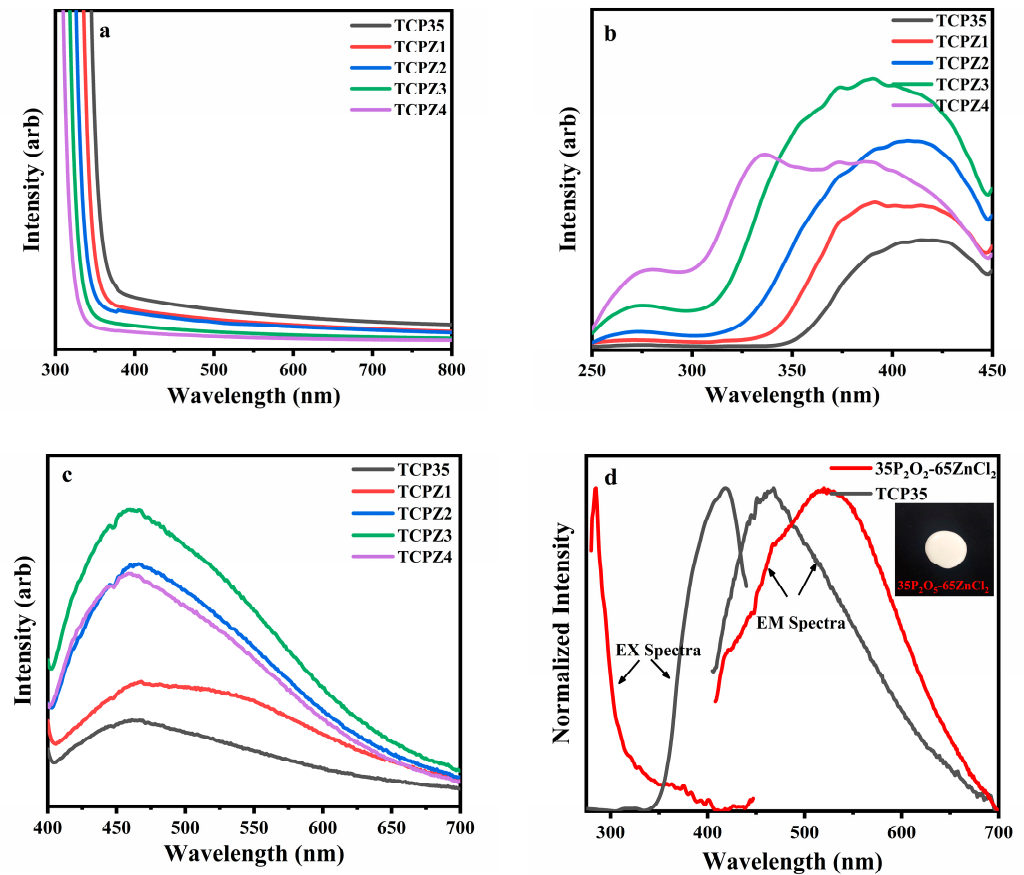


Figure 4. DSC curves (a) and Raman spectra (b) of TCPZ glasses.

Figure 5a shows the absorption spectra of the TCPZ glasses, in which the transparency increases and the UV absorption edges blue-shift with increasing  $\text{ZnCl}_2$  content. Figure 5b shows the PLE spectra of the TCPZ glasses when the excitation wavelength is 530 nm. Like the TCP glasses, the excitation band at approximately 275 nm is almost unchanged. However, the long absorption bands blue-shift and broaden with increasing  $\text{ZnCl}_2$  content. The  $\text{Sn}^{2+}$  ions are dispersed after the  $\text{Zn}^{2+}$  ions enter the TCPZ glasses, which changes the coordination field of  $\text{Sn}^{2+}$  and increases the asymmetry of the next nearest neighbor of  $\text{Sn}^{2+}$ , broadening the PLE spectra. However, the covalency of Zn-Cl bonds is lower than that of Sn-Cl bonds; therefore, the charge density in the glass structure decreases with increasing Zn-Cl bonds, resulting in broadening band-gap and blue shifts of the absorption and PLE spectra.

Figure 5c shows the PL spectra of the TCPZ glasses when the excitation wavelength is 390 nm. The luminescence intensities of the TCPZ glasses first increase and then decrease with increasing  $\text{ZnCl}_2$  content. Among them, the luminescence intensity of the TCPZ3 glass is the highest, and approximately four times that of the binary TCP35 glass. The addition of  $\text{ZnCl}_2$  not only increases the luminescence of the  $\alpha$ -band at 450 nm, but also increases the luminescence of the  $\beta$ -band at 530 nm. To explore the action of  $\text{ZnCl}_2$  on increasing the luminescence, the  $35\text{P}_2\text{O}_5\text{-}65\text{ZnCl}_2$  (P-Zn) sample was melted at  $350\text{ }^\circ\text{C}$  and then quickly cooled, and an opaque glass-ceramic (Figure 5d) was obtained. Figure 5d shows the PLE-PL spectra of the binary P-Zn and P-Sn samples. The P-Zn samples exhibit a strong excitation band at 285 nm, which may originate from the charge transfer of Zn-O [24]. It also exhibits a green broadband visible luminescence when excited at 390 nm, which may be due to intrinsic defects in the samples [25]. However, it should be noted that the P-Zn sample is not only opaque but also has high hygroscopicity, whose spectral properties are significantly affected with time. For three reasons,  $\text{ZnCl}_2$  plays a significant role in improving the luminescence of the glass. First, the introduction of  $\text{ZnCl}_2$  reduces the visible-light absorption of the TCP glasses; second, it improves the dispersion of  $\text{Sn}^{2+}$  ions, significantly enhancing the luminescence of the  $\alpha$ -band. Finally,  $\text{Zn}^{2+}$  increases the

luminescence of the TCP glasses at 530 nm, and an energy exchange may occur between  $\text{Sn}^{2+}$  and  $\text{Zn}^{2+}$  in TCPZ glasses, thereby increasing the luminescence intensity.



**Figure 5.** (a) Absorption spectra; (b) PLE spectra under 530 nm excitation; (c) PL spectra of TCPZ glasses under 390 nm excitation; (d) PLE-PL spectra of TCP35 and  $35\text{P}_2\text{O}_5\text{-}65\text{ZnCl}_2$  glasses. The inset is the physical image of binary P-Zn glasses.

Figure 6a shows the fluorescence decay curve of the TCPZ samples; the decay time of the samples increased only slightly with the introduction of  $\text{ZnCl}_2$ , but the change was not significant. It has been reported that the decay time of  $\text{Sn}^{2+}$  centers in zinc phosphate glasses is in the microsecond range, corresponding to the relaxation of the T1 to S0 states [19]. The decay times of  $\text{Sn}^{2+}$  in the TCPZ glasses are significantly shorter than those reported previously, mainly due to the high  $\text{Sn}^{2+}$  content in the TCPZ glasses. Generally, the decay time of tin-containing glasses decreases with increasing  $\text{Sn}^{2+}$  content [6]. The  $\text{SnCl}_2$  content is more than 20% in the TCPZ glasses, leading to the rapid decay of the glasses. Figure 6b shows the color chromaticity coordinates, physical photographs, and luminescence images of the TCPZ glasses excited by UV light at 365 nm. The ternary TCPZ glasses are colorless and transparent, and their luminescence shows different color-rendering properties when excited at 365 nm. Perfect white-light emission is obtained in the TCPZ2 and TCPZ3 samples with CIE coordinates of (0.3149, 0.3580) and (0.2811, 0.3306), respectively. This indicates that Sn-Zn chlorophosphate glasses without rare-earth elements can be used as white-light-emitting glasses and phosphors for UV LED chips.

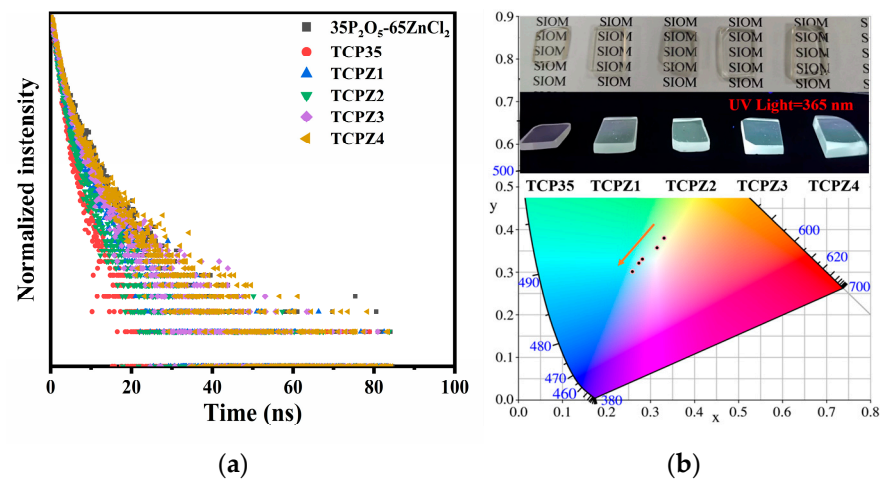


**Figure 6.** (a) Fluorescence decay curve of TCPZ glasses at 530 nm; (b) Color coordinates of the TCPZ glasses and photograph of the physical samples and luminescence under UV lamp excitation.

#### 4. Conclusions

TCP glasses prepared at 350 °C exhibit an intrinsic luminescence with a broadband luminescence of 400–700 nm under excitation at 380–430 nm. Compared to tin fluoride-phosphorous glasses, the excitation wavelength peak of tin chlorophosphorous glasses is red-shifted and broadened due to the covalence of the Sn-F bond being lower than that of the Sn-Cl bond. Furthermore, the introduction of ZnCl<sub>2</sub> into tin chlorophosphate glasses can considerably enhance luminescence, but it does not affect their low-temperature characteristics, and luminescence intensity can be increased fourfold. The reason for the enhancement effect is considered to be that ZnCl<sub>2</sub> reduces the visible-light absorption, improves the dispersion of Sn<sup>2+</sup> ions, and increases the luminescence of TCPZ glasses at 530 nm; moreover, an energy exchange may occur between Sn<sup>2+</sup> and Zn<sup>2+</sup> in TCPZ glasses.

**Author Contributions:** Conceptualization, T.W. and D.C.; methodology, T.W.; validation, T.W., Y.T., P.W. and M.Z.; formal analysis, T.W.; investigation, T.W.; resources, Y.T.; data curation, P.W.; writing—original draft preparation, T.W.; writing—review and editing, T.W. and D.C.; visualization, T.W.; supervision, D.C.; project administration, D.C.; funding acquisition, D.C. All authors have read and agreed to the published version of the manuscript.

**Funding:** This research was funded by the National Natural Science Foundation of China (Grant No. 51872308).

**Institutional Review Board Statement:** Not applicable.

**Informed Consent Statement:** Not applicable.

**Data Availability Statement:** Not applicable.

**Conflicts of Interest:** The authors declare no conflict of interest.

#### References

1. Nakanishi, T.; Tanabe, S. Novel Eu<sup>2+</sup>-Activated Glass Ceramics Precipitated with Green and Red Phosphors for High-Power White LED. *IEEE J. Sel. Top. Quantum Electron.* **2009**, *15*, 1171–1176. [[CrossRef](#)]
2. Yoo, H.; Kouhara, Y.; Yoon, H.C.; Park, S.J.; Oh, J.H.; Do, Y.R. Sn-P-F containing glass matrix for the fabrication of phosphor-in-glass for use in high power LEDs. *RSC Adv.* **2016**, *6*, 111640–111647. [[CrossRef](#)]
3. Karadza, B.; Van Avermaet, H.; Mingabudinova, L.; Hens, Z.; Meuret, Y. Efficient, high-CRI white LEDs by combining traditional phosphors with cadmium-free InP/ZnSe red quantum dots. *Photonics Res.* **2022**, *10*, 155–165. [[CrossRef](#)]
4. Masai, H.; Takahashi, Y.; Fujiwara, T.; Matsumoto, S.; Yoko, T. High Photoluminescent Property of Low-Melting Sn-Doped Phosphate Glass. *Appl. Phys. Express* **2010**, *3*, 082102. [[CrossRef](#)]
5. Masai, H.; Fujiwara, T.; Matsumoto, S.; Takahashi, Y.; Iwasaki, K.; Tokuda, Y.; Yoko, T. White light emission of Mn-doped SnO-ZnO-P<sub>2</sub>O<sub>5</sub> glass containing no rare earth cation. *Opt. Lett.* **2011**, *36*, 2868–2870. [[CrossRef](#)] [[PubMed](#)]

6. Masai, H.; Tanimoto, T.; Fujiwara, T.; Matsumoto, S.; Tokuda, Y.; Yoko, T. Correlation between emission property and concentration of Sn<sup>2+</sup> center in the SnO-ZnO-P<sub>2</sub>O<sub>5</sub> glass. *Opt. Express* **2012**, *20*, 27319–27326. [[CrossRef](#)]
7. Zhang, T.J.; Zhou, C.C.; Lin, J.; Wang, J. Effects on the emission discrepancy between two-dimensional Sn-based and Pb-based perovskites. *Chin. Opt. Lett.* **2022**, *20*, 021602. [[CrossRef](#)]
8. Wang, Y.J.; Yu, Y.; Zou, Y.; Zhang, L.Y.; Hu, L.L.; Chen, D.P. Broadband visible luminescence in tin fluorophosphate glasses with ultra-low glass transition temperature. *RSC Adv.* **2018**, *8*, 4921–4927. [[CrossRef](#)]
9. Wang, Y.J.; Li, Y.; Han, S.; Zhang, L.Y.; Chen, D.P. Continuously tunable broadband emission of Mn<sup>2+</sup>-doped low-melting point Sn-F-P-O glasses for warm white light-emitting diodes. *J. Am. Ceram. Soc.* **2018**, *101*, 5564–5570. [[CrossRef](#)]
10. Mao, W.; Cai, M.Z.; Xie, W.Q.; Li, P.P.; Zhen, W.Y.; Xu, S.Q.; Zhang, J.J. Tunable white light in trivalent europium single doped tin fluorophosphates ultra-low melting glass. *J. Alloys Compd.* **2019**, *805*, 205–210. [[CrossRef](#)]
11. Wang, R.; Zhang, J.H.; Zhang, Y.J.; Lin, H.; Pun, E.Y.B.; Li, D.S. Phosphor-in-glass with full-visible-spectrum emission based on ultra-low melting Sn-F-P-O glass pumped by NUV LED chips. *J. Alloys Compd.* **2021**, *864*, 158671. [[CrossRef](#)]
12. Jiang, S.B.; Luo, T.; Wang, J.F. Spectral properties of organic chromophores in fluorophosphate glasses. *J. Non-Cryst. Solids* **2000**, *263*, 358–363. [[CrossRef](#)]
13. Wu, T.; Wang, C.; Shen, Y.; Du, Y.; Tao, Y.; Wang, P.; Chen, D. Preparation and structure of low-melting-point stannous chlorophosphate containing nitrogen glasses. *J. Non-Cryst. Solids* **2022**, *591*, 121739. [[CrossRef](#)]
14. Skuja, L. Isoelectronic Series of Twofold Coordinated Si, Ge, and Sn Atoms in Glassy SiO<sub>2</sub>—A Luminescence Study. *J. Non-Cryst. Solids* **1992**, *149*, 77–95. [[CrossRef](#)]
15. Masai, H.; Yamada, Y.; Suzuki, Y.; Teramura, K.; Kanemitsu, Y.; Yoko, T. Narrow Energy Gap between Triplet and Singlet Excited States of Sn<sup>2+</sup> in Borate Glass. *Sci. Rep.* **2013**, *3*, 3541. [[CrossRef](#)] [[PubMed](#)]
16. Shen, C.; Ou, Y.; Qin, G.; Chen, G.; Baccaro, S. Optical properties of phosphate glass containing SnO<sub>2</sub>. *Glass Technol. -Eur. J. Glass Sci. Technol. Part A* **2010**, *51*, 213–215.
17. Mao, W.; Xie, W.Q.; Li, P.P.; Lu, Y.; Duan, Y.M.; Xu, S.Q.; Zhang, J.J. Double relaxation emission of Sn<sup>2+</sup> activator in tin fluorophosphate glass for device applications. *Chem. Eng. J.* **2020**, *399*, 125270. [[CrossRef](#)]
18. Masai, H.; Fujiwara, T.; Matsumoto, S.; Takahashi, Y.; Iwasaki, K.; Tokuda, Y.; Yoko, T. High efficient white light emission of rare earth-free MnO-SnO-ZnO-P<sub>2</sub>O<sub>5</sub> glass. *J. Ceram. Soc. Jpn.* **2011**, *119*, 726–730. [[CrossRef](#)]
19. Torimoto, A.; Masai, H.; Okada, G.; Yanagida, T. X-ray induced luminescence of Sn<sup>2+</sup>-centers in zinc phosphate glasses. *Radiat. Meas.* **2017**, *106*, 175–179. [[CrossRef](#)]
20. Hudgens, J.J.; Brow, R.K.; Tallant, D.R.; Martin, S.W. Raman spectroscopy study of the structure of lithium and sodium ultraphosphate glasses. *J. Non-Cryst. Solids* **1998**, *223*, 21–31. [[CrossRef](#)]
21. Zhang, L.Y.; Li, H.; Hu, L.L. Statistical structure analysis of GeO<sub>2</sub> modified Yb<sup>3+</sup>: Phosphate glasses based on Raman and FTIR study. *J. Alloys Compd.* **2017**, *698*, 103–113. [[CrossRef](#)]
22. Thuat, N.T.; An, N.M.; Nguyen, K.D.; Nguyen, T.D.; Truong, T.T. Synthesis of organo tin halide perovskites via simple aqueous acidic solution-based method. *J. Sci. Adv. Mater. Devices* **2018**, *3*, 471–477. [[CrossRef](#)]
23. Moreira, E.; Henriques, J.M.; Azevedo, D.L.; Caetano, E.W.S.; Freire, V.N.; Albuquerque, E.L. Structural, optoelectronic, infrared and Raman spectra of orthorhombic SrSnO<sub>3</sub> from DFT calculations. *J. Solid State Chem.* **2011**, *184*, 921–928. [[CrossRef](#)]
24. Jain, D.; Sudarsan, V.; Vatsa, R.K.; Pillai, C.G.S. Luminescence studies on ZnO-P<sub>2</sub>O<sub>5</sub> glasses doped with Gd<sub>2</sub>O<sub>3</sub>:Eu nanoparticles and Eu<sub>2</sub>O<sub>3</sub>. *J. Lumin.* **2009**, *129*, 439–443. [[CrossRef](#)]
25. Djuricic, A.B.; Leung, Y.H.; Tam, K.H.; Ding, L.; Ge, W.K.; Chen, H.Y.; Gwo, S. Green, yellow, and orange defect emission from ZnO nanostructures: Influence of excitation wavelength. *Appl. Phys. Lett.* **2006**, *88*, 103107. [[CrossRef](#)]